Lasers Manuf. Mater. Process. (2015) 2:164–185
DOI 10.1007/s40516-015-0013-4

Laser Assisted Milling of Ti-6Al-4V ELI with the Analysis of Surface Integrity and its Economics

Gary K. Hedberg[1] · **Yung C. Shin**[1]

Accepted: 23 June 2015 / Published online: 8 July 2015

Abstract This study presents the experimental evaluation of laser assisted milling (LAML) of Ti-6AL-4V ELI (Ti-64), which is used in the orthopedic industry, by using localized preheating of the workpiece via laser irradiation. Improvements to the machinability of this material with LAML are assessed while considering the surface integrity. Suitable laser heating conditions as well as machining conditions are determined based on temperature prediction modeling. Machinability improvements are shown in terms of tool wear, material removal rates and cutting force reduction. Systematic characterization of samples is shown to demonstrate that the machined sub-surfaces are not adversely affected during LAML by precisely controlling laser heating, via hardness measurements, scanning electron microscopy (SEM) for microstructure analysis, and X-ray diffraction (XRD) for residual stresses. An economic analysis shows that LAML provides the cost reduction over conventional machining.

Keywords Laser-assisted milling · Titanium alloy · Thermal analysis · Machinability improvement · Surface integrity

Introduction

One material that continues to see applications for improved part performance is titanium. This material provides unique benefits and increasing applications as a result of its distinct material properties. Titanium alloys have high strength-to-weight ratios and are very corrosion resistant. Ti-6Al-4V ELI, grade 23, is an alloy that is used in the biomedical industry to create implants, offshore oil and gas production industries for parts in seawater and the chemical industry for cryogenic containers [1, 2]. The same

✉ Yung C. Shin
shin@purdue.edu

[1] Center for Laser Based Manufacturing, School of Mechanical Engineering, Purdue University, West Lafayette, IN 47907, USA

properties that make titanium alloys attractive for various applications also make these materials very difficult to machine at room temperature due to excessive tool wear.

The problems associated with machining of Ti-6Al-4V alloys can be summarized using the following key points:

- High thermal stresses at the tool cutting edge due to low heat dissipation by chips and workpiece (cutting temperature is twice as high as that of steel Ck45, thus enhancing diffusion and adhesion, and causing high temperature gradients to occur, which result in thermal stress within the tool)
- High pressure load on the cutting edge (low plasticity of Ti-6Al-4V reduces chip contact length on the tool and at high cutting speeds it increases further due to "decreasing shearing angle")
- Tool failure by chipping due to high cutting forces and self-induced chatter
- Low clearance angle due to material spring back as a result of low Young's modulus and high yield stress (which increases friction and chatter)
- Vibration affinity due to low Young's modulus
- Diffusion based wear due to high reactivity of titanium
- Strong affinity for adhesion due to heat buildup in the cutting zone
- Potential exoergic reaction of titanium chips with atmospheric oxygen

Several common practices for milling Ti-6Al-4V ELI have been found to help improve tool wear. These include increasing the rigidity of the setup, using downmilling, and ensuring a constant feed once the tool is engaged in the workpiece. Each of these reduces the amount of chatter and heat build-up on the cutting tool and improves tool life [3].

Some previous studies showed how to improve the machinability of titanium alloys in terms of tool materials and coating technologies [4–6]. Since titanium machining is mostly carried out in industry with use of a coolant, alternative types of coolant supplying techniques were considered such as high pressure coolant [7, 8] and minimum quantity lubrication (MQL) techniques [9, 10] with varying degrees of success. One study on Ti-6Al-4V alloy machining using a high pressure coolant achieved good results during drilling with TiAlN coated tools at twice the normal cutting speed, but found only slight improvements during turning with uncoated carbide tools [7]. Another study on Ti-6Al-4V alloy turning using carbide and CBN cutting tools showed that there was an increase in tool life as a result of using a high pressure coolant during machining, but cubic boron nitride (CBN) cutting tools did not perform as well as typical carbide tools [8]. A study on MQL drilling, using synthetic ester and palm oils, resulted in a reduction of overall tool wear compared with dry machining [9]. One study on the benefits of MQL milling of a Ti-6Al-4V alloy using vegetable oil created a substantial increase in tool life over dry and traditional cooling methods [10]. Recently Bermingham et al. [11] carried out a comparative study of different cooling schemes of dry cutting, flood cooling and MQL along with the laser assisted milling and concluded that MQL with and without laser-assist performed better at higher speeds, while flood cooling worked at a low speed recommended by the manufacturer. Despite these efforts and others, machining speed of titanium alloys is still limited to low speed because the types of tool material suitable for machining of titanium alloys are mostly uncoated and coated carbide tools.

Laser-assisted machining has emerged as one of the potential techniques to improve the machinability of titanium alloys and other difficult-to-machine materials. Laser-assisted machining has been successful in improving tool life for various materials such as Waspaloy [12], fiber and particulate reinforced metal matrix composites [13, 14], titanium alloys [15–17], and Inconel 718 [18]. Challenges are however introduced when attempting to use laser assisted machining for titanium alloys. Titanium alloys are categorized based on their microstructure and are divided into three main groups: α-alloys, β- alloys and α/β- alloys. Among the alloys, Ti-6Al-4V ELI belongs to the α/β- alloy group, which is known for its heat treatability and relatively low Young's modulus. This heat treatability introduces additional challenges when applying laser assisted machining.

Dandekar et al. [15] conducted a comparative experimental study for turning of Ti-6Al-4V alloy by conventional, laser-assist and hybrid machining that employs simultaneous laser heating of workpiece material and liquid nitrogen cooling of the cutting tool. It was shown that the greatest success could be achieved using the hybrid technique when compared with LAM and liquid nitrogen alone. This testing showed that laser parameters could be used such that they would not alter final material properties compared with traditional turning. Rashid et al. [16] investigated the influence of laser power on LAM of Ti-6Cr-5Mo-5V-4A, which is a β alloy. It was found that low laser power did not significantly reduce cutting force during turning, while high laser power resulted in detrimental chip pile-up and poor tool wear characteristics. It was suggested to use the medium laser power range of 800–1200 W with the cutting speed range of 55–100 min to avoid any detrimental effects.

The above studies were focused on turning. Milling is however a more versatile process as it can be used to produce many complex parts with arbitrary geometry. Since milling is an interrupted process with continual rotation of the cutter, there are some potential challenges in implementing laser assisted milling. Some recent studies have shown successful results of laser-assisted milling in micro scale [19–21] and macro scale [22–27]. Shelton et al. [19, 20] carried out laser assisted micro-milling on difficult-to-machine materials of AISI 316, AISI 422, Ti-6Al-4V and Inconel 718 using side milling and slotting configurations. Improvements were found in surface finish on the final workpiece along with a reduction of edge burrs and a reduction in cutting force as indicated by AE sensor readings.

Tian et al. [22], Yang et al. [23] and Wiedenmann et al. [24, 25] presented modeling of temperature prediction during laser-assisted milling, which was subsequently used to design the process and determine the heat-affected zone. Ding et al. [21] performed the combined thermal and mechanical modeling during laser assisted micro-milling of 422 SS, Inconel 718, and Ti-6Al-4V with a good experimental validation of the simulation results. Brecher et al. [26] integrated a laser into a milling machine spindle and performed LAML experiments on an Inconel 718 workpiece and showed that the overall tool life could be improved through coordination of laser heating during tool rotation and workpiece interaction. Sun et al. [27] presented the experimental work on LAML of a Ti-6Al-4V alloy using up-milling and showed a reduction of cutting force and reduced tool wear over conventional machining. The thermal modeling was carried out using a simple analytical solution to determine the temperature of the workpiece at a point on the top surface and a point at the depth of cut during the laser heating process. They also showed that too high laser power would result in melting of the

workpiece surface, which would produce chipping of the insert as the tool interacted with this material.

LAML is investigated in this study for machining of Ti-6Al-4V ELI grade 23 to determine how machinability can be improved and machining costs can be reduced. While many studies have been carried out on various difficult-to-machine materials, no study dealt with this specific alloy. Different compositions are likely to produce different results even among titanium alloys. Therefore, this study focuses on how much machinability can be improved without creating any adverse effects on the final workpiece for a material that is heat treatable. Modeling work is used to determine the temperature distribution during laser-assisted milling to design suitable operating parameters. Although similar modeling was performed to predict when a heat affected zone will appear on the workpiece surface [23, 24], the current modeling work focuses on determining laser parameters that will avoid such damage and characterizing the potential benefits of LAML. A detailed surface integrity analysis is performed on the machined workpiece to determine the influence of laser parameters on final part properties. An economic analysis is also performed for laser assisted milling to demonstrate the cost benefits of LAML over traditional machining without any adverse effects on finished material.

Experimental Procedure

Milling experiments were performed on a MAZAK VQC-40/15 vertical milling center with a MAZATROL- M32 controller. The machine has a maximum spindle speed of 6000 rpm. A fiber laser with the wavelength of 1.071 μm (IPG Photonics Ytterbium laser: YLS-1000) was used, which produces a maximum output power of 1.0 kW. The focal length of the lens was 401 mm, and the final spot size was 2.6×3.6 mm in an elliptical shape with a Gaussian distribution.

A Kennametal Mill 1–14 tool holder (Kennametal M1D075E1402W075L175) with TiAlN coated carbide grade inserts (KC725M) was used during machining tests of Ti-6Al-4V ELI workpieces. The combined geometry of the tool and insert results in a 19.05 mm diameter, 0° lead angle, 15° radial rake, 3° axial rake, and a nose radius of 0.8 mm for the cutting tool. Fly cutting was used during all the tool wear and force tests to avoid potential issues with runout. Downmilling was used in all machining experiments with a face milling configuration. A flood coolant was applied during traditional machining experiments, which consisted of a 10 % mixture of oil and water. An assist gas of argon was used in LAML to keep the chips away from the laser delivery optics and reduce the possibility of fire within the experimental setup. The overall schematic of the experimental set-up is shown in Fig. 1.

A Kistler 3 component dynamometer type 9257B with a Kistler 5004 dual mode amplifier was used to measure cutting force data. Labview software was used to collect data from the amplifier with a sampling rate of 2 kHz during machining of Ti-6Al-4V ELI. Tool wear measurements were taken using a Nikon Eclipse LV150 optical microscope and analyzed using a SPOT Insight Firewire software and camera.

For microscopic examination, the machined Ti-6Al-4V ELI samples were sectioned and prepared using 320, 400, 600, 800 grit papers and polished using a colloidal silica of 6 and 0.5 μm on a polishing wheel, according to standard metallographic techniques.

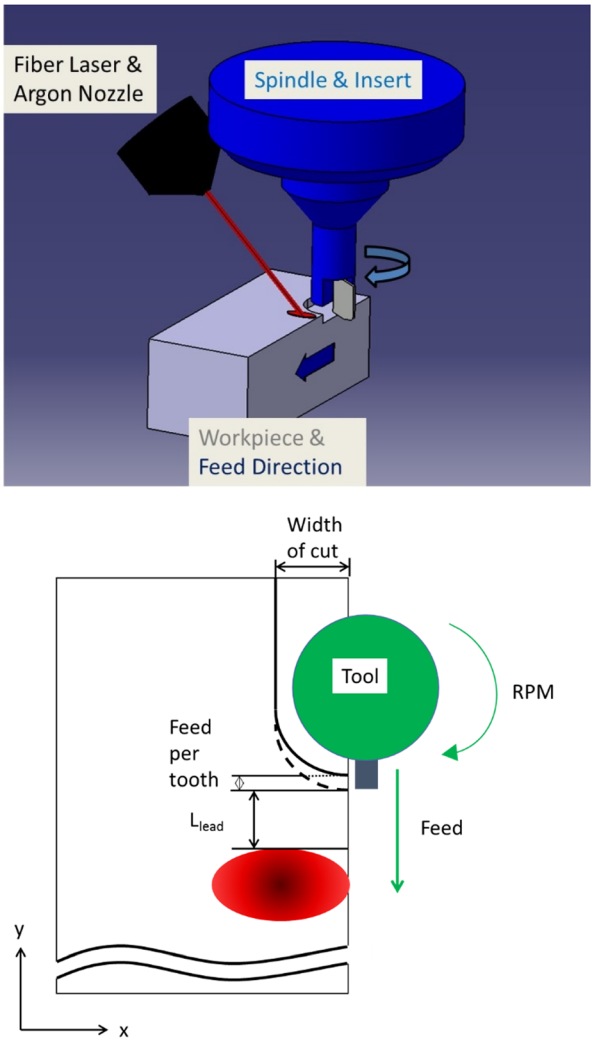

Fig. 1 General Machining Setup for LAML

All samples were etched using Kroll's Reagent (ASTM 192), and images were taken using the Nikon Eclipse LV150 optical microscope and a JEOL T330 SEM.

A Mitutoyo hardness tester (model ATK F1000) was used to determine the surface hardness in the HRC scale using 150 kgf, and a 120° diamond cone indenter. All measurements were taken on the final workpiece surface. Microhardness analysis was performed using a LECO KM 247AT machine and hardness was recorded using a Vickers hardness scale using a 200 g load and a dwell time of 13 s. Measurements were taken at specific depths below the machined surface to determine the change in hardness with respect to distance. Hardness at a very shallow depth could not be measured accurately as the workpiece would deform when the indenter was too close to the edge.

A Bruker D8 Focus X-Ray diffractometer was used for XRD analysis of Ti-6Al-4V ELI samples, which has a Cu-K(α) source, a 3 circle goniometer, and a Lynseye 1D detector. A scan step of 0.024° was used with a counting time of 8 °/min.

Residual stresses were measured on the Ti-6Al-4V samples using the X-ray diffraction technique on Bruker D8 Discover X-Ray Diffractometer with General Area Detector Diffraction System (GADDS) using Cr-K(α) radiation (λ=0.22897 nm) at 30 kV, 50 mA to acquire {103} diffraction peaks at 2θ angles of about 119.3° using a spot of 0.8 mm collimated from the 2 mm beam. A two-dimensional approach was used to evaluate the 2D diffraction data. The data processing and stress evaluation were performed with GADDS software and Materials Data Incorporated's Jade, respectively. Depth profiles for the residual stresses were measured by chemically etching successive layers of the material by electropolishing using an etchant of 8 % HF and 92 % H_2O, with an etching interval of 40 s to remove 25 μm of material.

Thermal Modeling

A transient, three-dimensional thermal model of a rectangular workpiece undergoing laser heating and material removal developed at Purdue University was used to predict the temperature distribution within the workpiece during LAML. Based on the temperature prediction, suitable operating parameters in terms of laser power and cutting conditions were determined to avoid any thermal damage and microstructural changes. A detailed description, including governing heat transfer equations, boundary conditions, and numerical scheme, is referred to Tian et al. [22].

An implicit finite volume method is used to discretize the governing equations and obtain a numerical solution. The modeled domain is divided into predefined control volumes with a 100×80×55 mesh in the x, y, and z directions for a workpiece with dimentions of 30×10×15 mm^3. Modeling of the LAML process was performed using thermal properties for a Ti-6Al-4V ELI workpiece for 10 s until a quasi-steady state was established. For the face milling configuration, the laser and tool feed directions were defined in the x-direction, with modeling performed using conduction, convection, radiation, and material removal. It is known from other work [19] that conduction plays the most important role in modeling the LAML process, but convection and radiation were included, since it did not significantly affect computational time. An example of thermal model temperature prediction for the workpiece is included in Fig. 2. Laser settings of 3 mm lead, 2.6×3.6 mm elliptical beam shape, 175 W power were used for a 1.2 mm/s feed and 3 mm width of cut in the example.

Material Properties

To obtain an accurate temperature prediction for the workpiece, correct material properties are required. For the experiments performed, a Ti-6Al-4V ELI alloy was used that met the AMS 4931 specifications. Details of the material composition are included in Table 1 and Table 2. Material properties were obtained from literature and functions were fitted to the temperature dependent data for thermal conductivity and specific heat (Table 3). Optical properties of emissivity (0.25) and absorptivity (0.35) for a Ti-6Al-4V alloy to an Nd:YAG laser (wavelength of 1060 nm) were found from

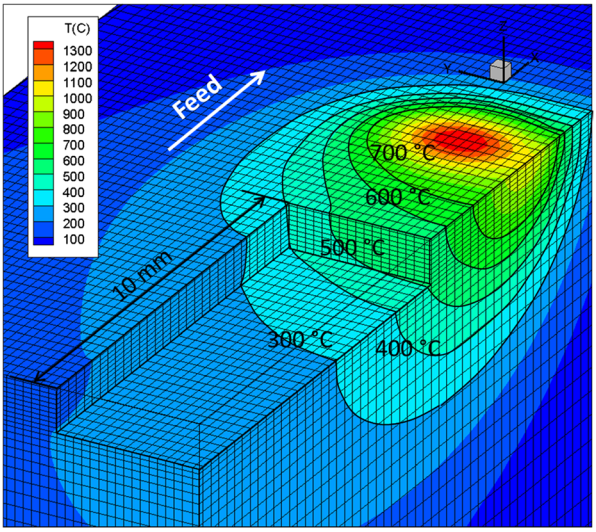

Fig. 2 Example Thermal Model Output for LAML of Ti-6Al-4V ELI for 175 W in Laser Power

literature [23] and were compared with experimental results for laser absorptivity to the fiber laser (wavelength of 1070 nm). A good agreement was found between the material absorptivity value from literature for a Nd:Yag laser wavelength (α=0.35) with the experimental results of workpiece laser absorptivity for a fiber laser wavelength in the low laser power range between 40 W and 90 W.

It was found that oxidation of the surface became apparent for high laser power above 90 W, which affected absorptivity. Absorptivity tests conducted showed that under the laser power of 90 W or below, the workpiece absorptivity was about 0.35, while the absorptivity value increased to 0.5 once surface oxidation occurs above 90 W of laser power. Modeled temperature prediction with these absorptivity values and surface temperatures measured by an infrared camera agreed well, as shown in Fig. 3.

Modeling Results

The thermal model was used to determine temperatures in the material removal zone ($T_{mr\text{-}ave}$), maximum workpiece surface temperature (T_{max}) and maximum temperature on the depth of cut plane ($T_{machined}$). A parametric relationship was then determined for these temperatures in terms of laser power (P) and feed rate (f). A full factorial design was used to obtain temperatures for typical machining speeds for Titanium alloys as

Table 1 Composition of Workpiece for AMS 4931 specifications

Element	Al	V	Fe	O	C	N	H	Y	Other—Total	Ti
Min	5.50	3.50	–	–	–	–	–	–	–	balance
Max	6.50	4.50	0.25	0.13	0.08	0.03	0.0125	0.005	0.3	

Table 2 Physical properties of Ti-6Al-4V (from [23, 28])

Density—ρ (kg/m^3)	Young's Modulus—E (Pa)	Poisson's Ratio	Emissivity	Nd-Yag Absorptivity
4430	113*10^9	0.34	0.25	0.35

well as higher machining speeds. MiniTab statistical software was used to perform the multivariable regression analysis to obtain workpiece temperature equations based on laser and machining parameters. These equations were used to limit temperatures in the final workpiece and prevent a heat affected zone in the final part, which can result from laser heating.

The resultant predictive equations from the regression analysis are:

$$T_{mr-ave} = 32.017 * \frac{(\alpha P)^{0.772}}{(f)^{0.156}} \tag{1}$$

$$T_{\max} = 133.238 * \frac{(\alpha P)^{0.633}}{(f)^{0.099}} \tag{2}$$

$$T_{machined} = 94.492 * \frac{(\alpha P)^{0.721}}{(f)^{0.23}} \tag{3}$$

Appropriate laser power levels were calculated using feed for the machining experiments, absorptivity of the material, and ideal temperatures for $T_{machined}$ such that it would not induce a phase change in the Ti-6Al-4V ELI material. It was determined that a maximum $T_{mr\text{-}ave}$ of 500 °C would avoid a potential microstructural change on the final surface of the part after LAML.

For the higher machining speeds of 75 m/min and 100 m/min, it was determined that laser power close to 140 W would result in oxidation of the workpiece surface; therefore, the corresponding absorptivity value of 0.5 was used for laser power above this value. From the modeling work it was determined that laser power above 185 W would result in 800 °C threshold temperature on the final workpiece surface for a machining speed of 75 m/min. As a result, laser power was limited to 185 W and 200 W for 75 m/min and 100 m/min, respectively.

Table 3 Temperature Dependent Thermal Properties for Ti-6Al-4V (from [28])

Property	Equation	Approximation for
Conductivity—k (W/m-K)	1.00×10^{-5}*T^2−0.0012*T+6.6519	For T(K)>1300 k=22.0
Specific Heat—C_p (J/kg-K)	0.21*T+483.37	For T(K)>1200 C_p=735

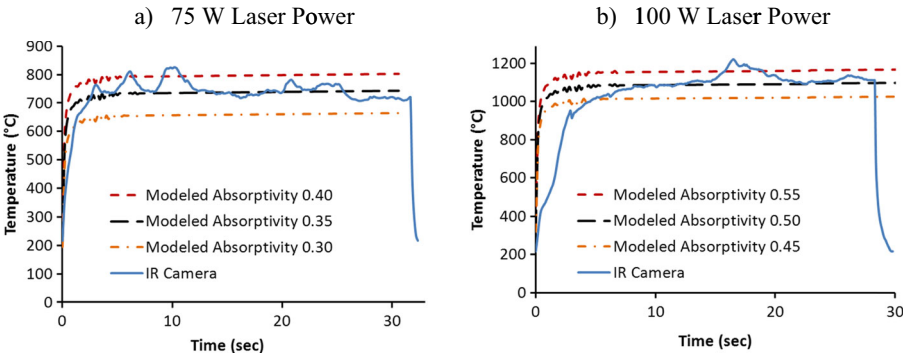

Fig. 3 IR camera results and thermal model calculation to determine workpiece absorptivity

A summary of the modeling results is presented in Fig. 4, with error bars representing the minimum and maximum temperature in the cutting zone. The dashed and broken lines respectively represent the critical temperatures in Ti-64 where phase change can begin (800 °C) and where surface oxidation begins (1100 °C). Based on the constraints established for the different machining speeds, it was observed that the surface of the final machined part could potentially be affected by the laser for $T_{mr\text{-}ave}$ values above 475 °C. A maximum $T_{mr\text{-}ave}$ of 500 °C was used in the tests to avoid possible microstructural change on the final surface of the part.

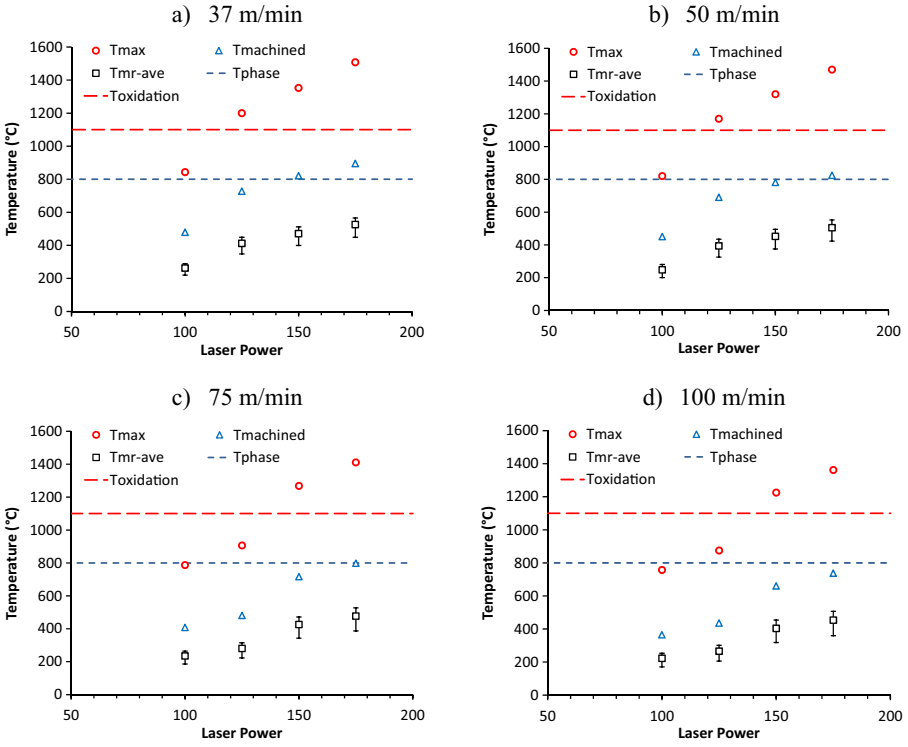

Fig. 4 Thermal model simulation results for LAML temperature prediction

Experimental Results

Cutting Force

A cutting speed of 75 m/min was used during machining experiments to characterize the influence of laser heating on cutting force so that an accurate comparison could be made between traditional machining and LAML using a face milling configuration. By reducing cutting force, it is likely that less deformation will occur on the machined components and tool life will be improved with the reduced pressure on the edge of the tool.

During the machining experiments, cuts were made along the 150 mm length of a Ti-6Al-4V ELI sample with the dimension of 150×125×50 mm^3. The machining parameters used included a cutting speed of 75 m/min, a feed of 0.1 mmpt, 1 mm depth of cut, and 3 mm width of cut. Laser parameters included a 2.6×3.5 mm^2 laser spot diameter, 3.5 mm laser lead distance, and a 41° angle of incidence measured from the horizontal direction.

Tests were performed with and without laser heating of the workpiece, as detailed in Table 4. To avoid any potential phase change in the final workpiece surface, a laser power of 180 W was used during LAML experiments based on the thermal modeling and regression analysis. It was calculated that this power would not increase the temperature at the final depth of cut location beyond the critical cutoff temperature chosen for the phase change, which is 880 °C, and it was determined that machining would be carried out with the $T_{mr\text{-}ave}$ of 500 °C.

Cutting force was recorded at the sample rate of 2 kHz. Examples of measured cutting force data are shown in Fig. 5, where F_y is the force in the feed direction and F_x is the force perpendicular to the feed direction. Peak force data was captured over the total length of cut, and an average peak cutting force was determined for each experiment. The summarized peak forces in both x and y directions for each experimental condition are given in Table 5. It was found that laser heating reduced peak cutting force by 20 and 23 % in the x and y directions, respectively, as shown in Fig. 6, with error bars representing one standard deviation in cutting force. From the LAML experiments it is clear that localized heating of the workpiece material reduces the cutting force during the machining process. Small cutting force observed between cycles was a result of tool rubbing against the workpiece surface, which is common during facemilling operations.

The 20 % reduction in cutting force measured during LAML of Ti-6Al-4V ELI is not as large as the 60 % reduction observed during milling of Inconel 718 [26] or the 40 % reduction during milling of a Ti-6Al-4V alloy [27]. This is mainly a result of differences in laser power and configurations during machining. Because the material

Table 4 Experimental Design for LAM of Ti-6Al-4V

Test	V (m/min)	Feed rate (mm/min)	Feed (mm/tooth)	RPM	P (W)	$T_{mr\text{-}ave}$ (°C)	T_{max} (°C)	$T_{machined}$ (°C)
Conv	75	125.3	0.1	1253	0	23	–	–
LAML	75	125.3	0.1	1253	180	500	1500	780

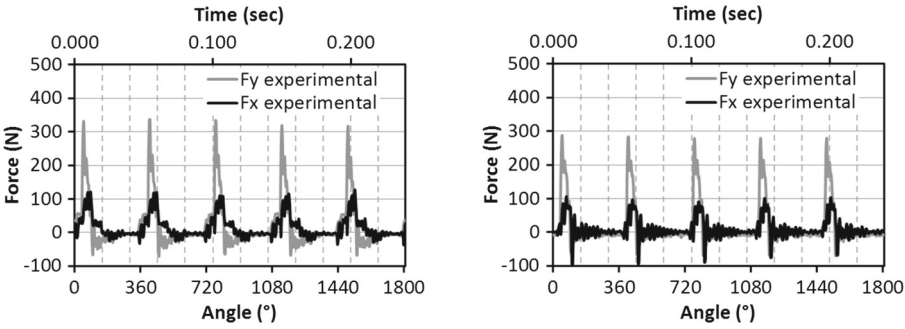

Fig. 5 Experimental cutting force during multiple tool rotations

properties of the final workpiece surface were of critical importance for the Ti-6Al-4V ELI alloy and the material is heat treatable by nature, laser power was limited during LAML experiments. This consideration was not included in the work presented by Brecher et al. [26] and Sun et al. [27]; therefore, with a higher laser power, a larger reduction in cutting force could be achieved.

Beam placement can also be a driving factor for the reduction in cutting force. The position of the laser beam relative to the cutting tool will influence the final temperature profile within the workpiece, which directly impacts the final cutting force that occurs during machining. For the current work, the more standard approach of delivering the laser beam to the workpiece ahead of the cutting tool was used for easy implementation.

Tool Wear

Tool wear tests were performed on the Ti-6Al-4V ELI workpiece using TiAlN PVD coated carbide inserts (Kennametal KC725M). Conventional milling tests were performed using a typical cutting speed of 50 m/min for titanium alloys, as well as higher speeds (65 and 75 m/min), to establish a baseline for overall tool life, using a flood coolant at all speeds. It was found that traditional milling at cutting speeds above 50 m/min would result in premature chipping of the tool during Ti-6Al-4V ELI machining. This chipping can occur on the flank or face of the insert, and reduces the predictability of tool life. Chipping is quite common when machining titanium alloys and has limited the cutting speed to 50 m/min and lower in industry.

Such chipping results in changes to insert geometry and can lead to a catastrophic tool failure during part production. As a result, conventional milling experiments were performed only until chipping was apparent on the tool. In order to compare tool life, a

Table 5 Experimental Matrix and Results of Milling of Ti-6Al-4V

Test	Laser Power (W)	Tmr-ave (°C)	F_x-Peak (N)	F_y-Peak (N)	F_x % decrease	F_y % decrease
Conv	–	–	120	333	–	–
LAML	180	250	100	270	20	23

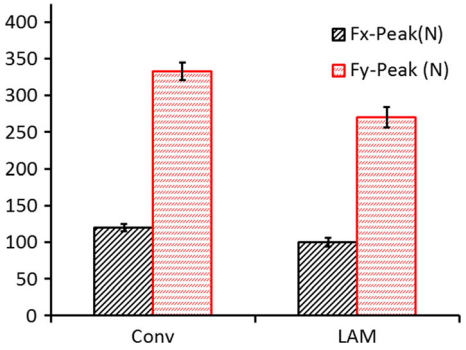

Fig. 6 Average peak cutting force results with error bars representing one standard deviation

critical cutoff value of 180 μm, although this is lower than typical values for other work materials, was used to define flank wear for the tool. This value minimized the role of chipping in overall tool life so that accurate tool wear trends could be calculated.

LAML experiments were performed on the Ti-6Al-4V ELI workpiece at a cutting speed of 75 m/min and 100 m/min without a coolant to determine the effect of LAML on overall tool life. Argon gas was applied to the cutting zone in experiments to remove chips from the tool and to protect the laser optics from potential damage. A total flow rate of 0.47 lpm at 0.35 MPa was delivered using two nozzles. The machining parameters used in tool wear testing are the same as those described in the cutting force experiments, with cutting speed and laser power modified based on modeling work performed. For tool life experiments, traditional machining (Conv1-Conv3) and LAML (LAM1-LAM2) were performed for machining speeds between 50 to 100 m/min. A summary of machining parameters is given in Table 6.

Unlike traditional machining, chipping was not present on the tools even at high cutting speeds during LAML. Testing was continued for LAML experiments until 225 μm of flank wear was measured. The elimination of premature chipping at high speeds during LAML provides a significant improvement over conventional milling. In order to accurately compare total tool lives between LAML and traditional milling, the lower critical value for flank wear of 180 μm was used to define the total tool life. Machining was performed for each machining speed with tool wear recorded at prescribed intervals until it reached the critical value as shown in Fig. 7.

From the results of tool life testing, there is a clear improvement when using LAML over traditional machining. The two main improvements are the slower progression of flank wear on the tool, and elimination of chipping at high cutting speeds during

Table 6 Tool Wear—experimental parameters

Test	V (m/min)	RPM	Feed (mmpt)	P (W)	$T_{mr\text{-}ave}$ (°C)	Coolant
Conv1	50	835	0.1	–	20	Oil based
Conv2	65	1086	0.1	–	20	Oil based
Conv3	75	1253	0.1	–	20	Oil based
LAM1	75	1253	0.1	185	500	None
LAM2	100	1671	0.1	195	500	None

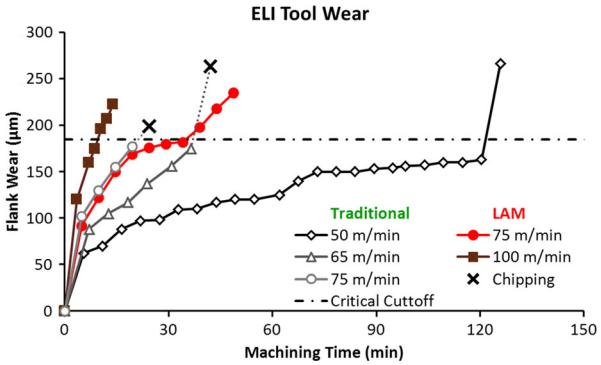

Fig. 7 Tool Wear Progression of KC725M Insert During Conventional Machining and LAML

LAML. Due to the increased tool life, an insert used for LAML will last 64 % longer than the one used for traditional milling. Alternatively, the cutting speed can be increased by 20 % when using LAML, compared with traditional milling, without reducing the total tool life of the insert. It was observed that LAML did not result in sudden chipping when flank wear is close to 180 µm. As a result, a higher margin of safety for tool failure is provided when using LAML at higher cutting speeds when compared with traditional machining. Both of these benefits can have a significant impact on part production time and total cost. Additional modification to laser parameters such as lead distance, spot size, and beam placement may further improve tool life. These modifications were not investigated due to setup constraints in this study.

To compare overall tool life for traditional milling and LAML, the Taylor tool life equation was used to characterize the failure of the tool as a result of flank wear. The failure of the tool was defined by flank wear that had exceeded 180 µm for a predictable tool life at all cutting conditions without premature chipping. This value is lower than the standard value typical for Ti tool wear; however, it ensures that accurate values are obtained for all tool life tests performed before chipping occurs. Using the 180 µm flank wear criteria, a Taylor tool life equation was established for both traditional milling and LAML of Ti-6Al-4V ELI, where cutting velocity V_c is in m/min and tool life T is in minutes:

$$\text{Conventional}: \; V_c T^{0.22} = 149 \tag{4}$$

$$\text{LAML}: \; V_c T^{0.22} = 168 \tag{5}$$

A log/log plot of tool wear experimental results with predictions by the Taylor tool life equations is shown in Fig. 8. The 20 % increase in cutting speed for the same amount of tool wear can be clearly seen.

Microstructural Analysis

The possibility of a heat affected zone in the final workpiece material necessitates an investigation of the final workpiece surface of Ti-6Al-4V ELI grade 23 after traditional machining and LAML. While a suitable laser level based on the required temperature

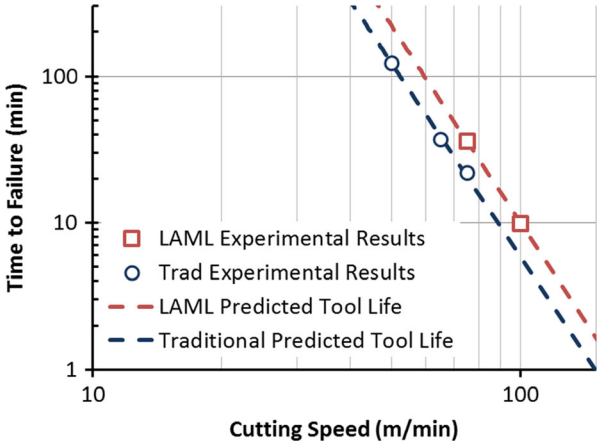

Fig. 8 Taylor tool life equations and experimental data for Ti-64 ELI

was chosen through thermal modeling, additional analysis must be performed to ensure that final workpiece properties are not adversely altered during the LAML process.

Optical Microscope Comparison

Images of the workpiece cross-section were obtained for traditional milling and LAML using 50 m/min and 75 m/min in cutting speed. A higher machining speed for LAML was used to ensure that the increased speed does not alter workpiece parameters beyond what is achieved during traditional milling at common cutting speeds. Unaltered material properties after LAML will indicate that increasing cutting speed as well as laser surface heating will not negatively influence final part properties.

Final part microstructure for LAML was determined using a comparison of grain size and orientation beneath the machined surface of sample parts. It was found that there was no difference in grain size directly below the machined surface of any of the cross sectioned samples (Fig. 9). The similarities appeared at the surface, and continued down to a deep depth (>2 mm) with grain orientation appearing to be random, with no specific orientation resulting from either traditional machining or LAML. It was concluded that no significant difference could be observed between the two samples, and that a heat-affected zone was avoided by using the thermal model temperature predictions.

SEM Analysis

SEM images were taken and compared for the traditional milling and LAML cross-sectioned samples to make a comparison of grain size and orientation on a smaller scale. The images show a microstructure of equiaxed and distorted α along with plate-like α is present with intergranular β through the entirety of the part, which is typical for the Ti-6Al-4V ELI grade 23 material that meets an AMS 4931 specification (Fig. 10). By observing the cross-section of the material, it was found that there was not a significant change in composition from the top of the machined surface all the way down to the bulk of the material (2 mm deep). As a result of optical microscope

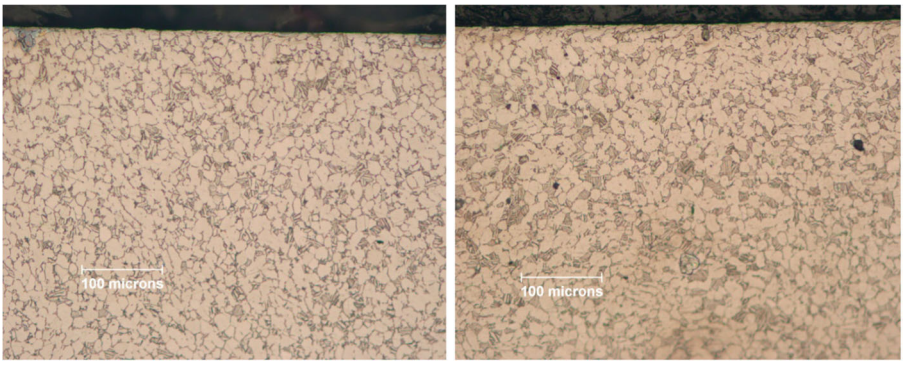

a) Traditional b) LAML

Fig. 9 Ti-6Al-4 V ELI Optical Microscope images from cross-sectioned samples etched with Kroll's reagent at 200x after traditional machining (**a**) and LAML (**b**)

and SEM images, it can be concluded that the LAML process parameters chosen did not produce a heat affected zone in the final workpiece.

XRD Analysis

It is known from other research that laser heating can be successfully applied to a Ti-6Al-4V alloy to change final part characteristics [29]. Although optical images and SEM images indicate that there is no significant microstructural change, non-destructive XRD analysis was performed on the top workpiece surface to ensure that phase change was avoided for this critical area. Samples did not receive any special preparation and had an average surface roughness of 0.3 μm. From literature [30–32], the standard way to characterize the 2θ peaks in Ti-6Al-4V is to use the JCPDS standard for titanium. The hexagonal α-Ti, and cubic β-Ti from the JCPDS standard (file #44–1294, and #44–1288, respectively) were used to determine where peaks should occur. These reference points are plotted along with the XRD experimental data (Fig. 11).

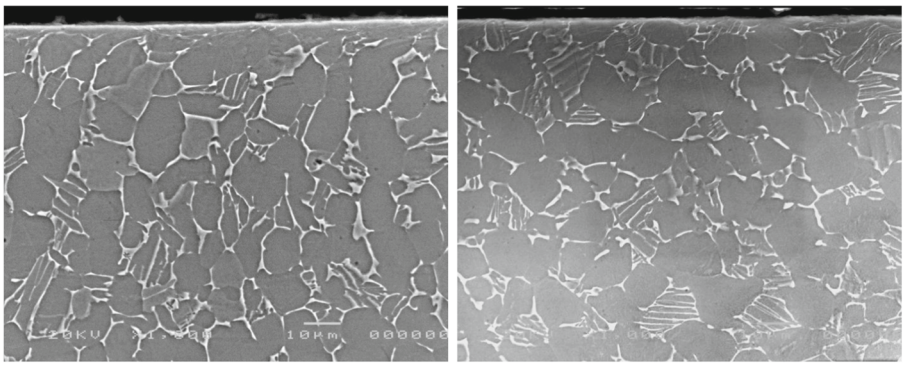

a) Traditional b) LAML

Fig. 10 SEM Images of etched Ti-6Al-4V sample at 1,000x (**a**) after traditional machining and (**b**) LAML

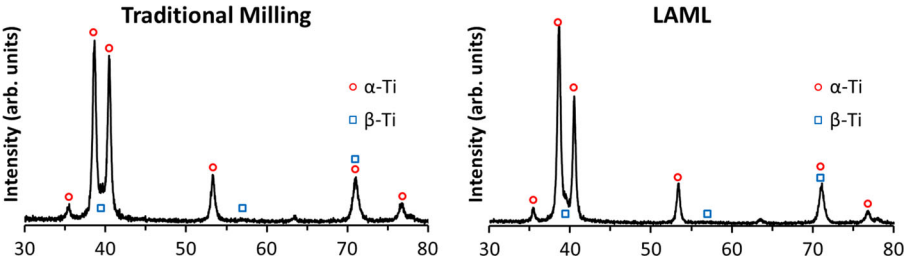

Fig. 11 XRD analysis for milling Ti-6Al-4V

Based on the results from XRD scans, it was determined that the machined surface of both samples mainly consist of α-phase Ti. This can be identified by observing that there are no significant peaks present for the β-phase Ti. It can be concluded that when appropriate laser power levels are used during LAML, a phase change can be avoided in the final workpiece surface. This conclusion is further reinforced through the SEM images, which show no significant differences in grain size and orientation between the samples machined using traditional machining methods and LAML.

Material Hardness

Material hardness testing was performed using a Mitutoyo hardness tester (model ATK F1000) for the initial Ti-6Al-4V ELI material, as well as for samples that had been processed using traditional machining and LAML. Figure 12 shows the average of 7 hardness tests for each sample with error bars to indicate the range of data.

Measurements showed a very slight decrease in the surface hardness of the final part for LAML, but it can be concluded from the XRD analysis this is not a result of a detrimental phase change. Common to traditional machining is an increase in surface hardness from grain size refinement and increased residual stresses. It has been shown that compressive residual stresses are generally observed during milling of titanium [33], which can result in a negative reduction of ductility on the part surface. After traditional machining, a separate stress relief heat treatment process may be needed to relieve this compressive residual stress.

The measured surface hardness was reduced by less than 10 % for the LAML samples when compared with traditional machining. As a result, the final hardness was within the range of hardness for the as-received material and all values were within the

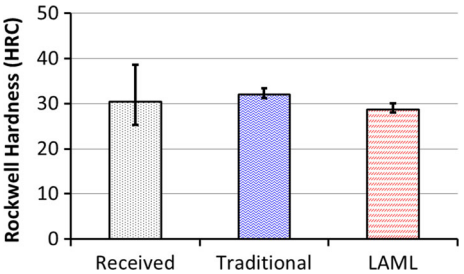

Fig. 12 Ti-6Al-4V ELI surface hardness results for the as-received material, traditional milling at 50 m/min, and LAML at 75 m/min (*error bars* for the range of data)

range of AMS 4931 specifications. The overall measured variations of final surface hardness for both types of machining were greatly reduced, when compared with those of the as-received material.

Due to the measured reduction of surface hardness in Fig. 12, a detailed investigation into microhardness was performed to determine if there was a significant alteration in hardness beneath the surface of the LAML workpiece. Microhardness tests were performed on the samples produced by LAML at 75 m/min and traditional milling at 50 m/min. Microhardness was analyzed at intervals of 100 μm for each sample down to a depth of 2 mm. It was determined that there was a relatively consistent hardness for both the samples by LAML and traditional machining through the depth of the workpiece. A gradual increase in hardness was observed close to the surface of the workpiece for both LAML and traditional milling experiments. This indicates that the surface hardness differences measured are limited to the very shallow top portion of the workpiece (Fig. 13). It is significant to note that there is no detrimental decrease in hardness of the workpiece as a result of LAML when compared with the bulk workpiece material.

Residual Stress

Residual stress analysis was performed on the machined samples for traditional milling at 50 m/min and LAML at 75 m/min. Measurements were taken in the feed and machining directions down to a depth of 200 μm, where stresses returned to zero. It was found that there was a slight reduction in compressive residual stresses on the surface of the workpiece as a result of the different machining processes as shown in Fig. 14. A 20 % reduction in residual stresses in the feed direction for LAML is apparent in Fig. 14b when compared with traditional machining; however, the depth of the material under compressive stresses are slightly higher for the workpieces produced by LAML.

When comparing the results of the residual stress analysis with surface hardness and micro-hardness measurements, it is clear that LAML induces slightly lower compressive residual stresses onto the workpiece during machining, which results in a slight decrease in surface hardness. The reduced residual stresses only affect a very shallow

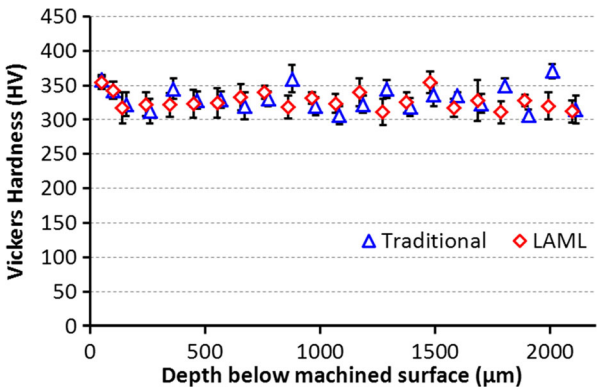

Fig. 13 MicroHardness results for traditional machining at 50 m/min and LAML at 75 m/min

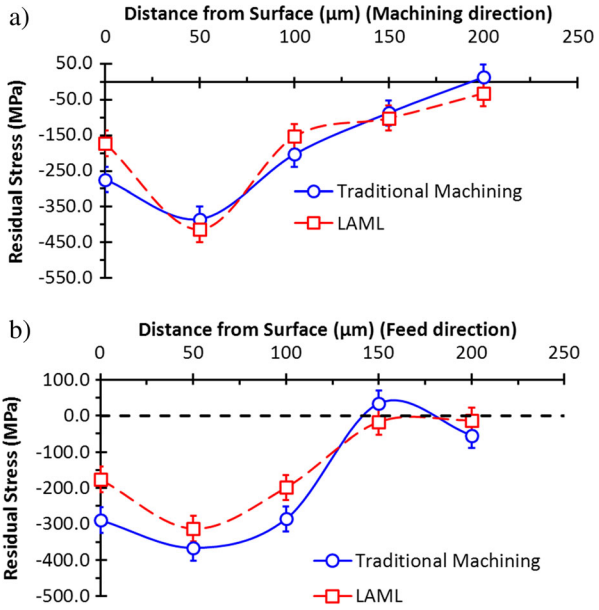

Fig. 14 Residual Stress measurement for Ti-6Al-4V after traditional machining at 50 m/min and LAML at 75 m/min for the machining direction (**a**) and feed direction (**b**)

portion of the machined workpiece and do not affect workpiece properties at deeper depths (below 200 μm). Final surface hardness measurements are closer to the bulk material hardness after LAML compared with traditional milling. As a result of all of the microstructural analysis performed on the final workpiece, it can be concluded that LAML can be performed without negatively influencing final workpiece properties.

Ti-6Al-4V ELI Economic Analysis

Because of the increase in tool life that can be achieved with LAML, a comparative cost analysis has been performed for LAML and traditional machining. This analysis uses the following assumptions:

- $200 per hour operation cost rate
- 3 min tool change time
- Tool cost: $17 per insert—2 cutting sides ($8.50 per tip)
- Part size: 4000 mm^3 (amount of material removed per part)
- At least one part made per tool
- Laser costs: $30 per hour for operation & depreciation

From the assumptions given and the Taylor tool life equations obtained from experimental tests, the total cost per piece was plotted for different cutting speeds during traditional machining with a coolant and LAML (Fig. 15). While the limitation of 50 m/min to cutting speed during traditional machining does not produce the minimum cost per part, it must be used in industry to prevent premature chipping

and potential damage to parts during machining. Since premature chipping does not occur during LAML, higher speeds are possible for part fabrication. As a result, the cost per part analysis for LAML can be performed at speeds that are optimized based on total machining costs.

The optimum cutting speed to minimize the total cost per part and maximize productivity of the machining center was determined for both traditional machining and LAML based on the experimented machining and laser parameters (Table 7). The increase from current traditional machining speeds of 50 m/min to 100 and 110 m/min for LAML indicates a significant increase in material removal and the total production rate of parts. There is also a 30 % reduction in cost per part when using LAML compared with traditional milling.

Because increases in cutting speed result in decreased total tool life, an increase in the amount spent per part for tool costs are increased. However, it is clear that LAML creates a significant improvement in both cost savings and production rate, despite the additional costs associated with the laser equipment and tool costs. It is important to note that results from this analysis are based off of the tool life equations calculated from a lower flank wear criteria, and non-optimized machining and laser parameters. Therefore the results presented here are not necessarily the best case scenario and a further improvement is possible.

A significant benefit that is not included in this economic analysis is the elimination of coolant during LAML. It is very difficult to calculate the true economic benefit to eliminating coolants due to the hidden costs of these fluids. These include the environmental impact of non-recyclable materials included in the coolant, health benefits to employees, etc. among others. Since these do not translate into a directly calculable cost, the desirable trait of coolant elimination of LAML is only discussed in this analysis.

The total machining cost for cutting one piece is shown in Fig. 16, with costs separated into their sources (laser, tool change, tool and operational costs). Optimum cutting speeds were used for both LAML and traditional milling to calculate the minimum cost and maximum productivity. As shown in Fig. 16, there is a 33 % reduction in cost for producing parts using LAML, even when taking into account the costs of the laser operation.

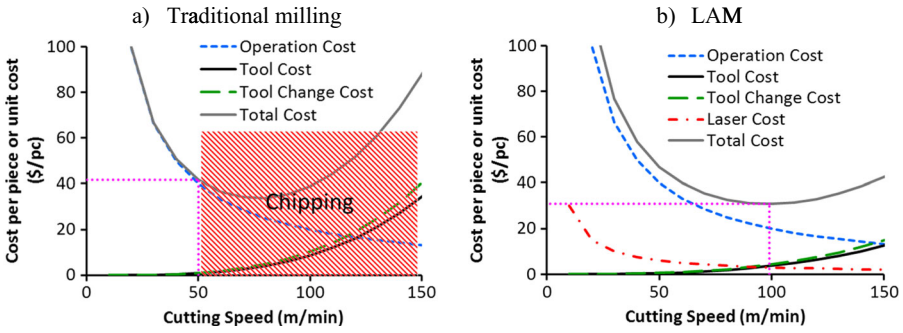

Fig. 15 Cost of producing one part based on Taylor tool life equations

Table 7 Optimized cutting speed based on Taylor tool life equations—Ti-6Al-4V ELI milling

Machining type	Optimized cutting speed	
	Min-cost (m/min)	Max-productivity (m/min)
LAM	100	110

Conclusions

Laser assisted milling was investigated to determine what benefits can be gained when machining Ti-6Al-4V ELI workpieces. Experiments performed using the laser parameters based on thermal modeling and material properties confirmed that the thermal modeling predicted workpiece temperatures accurately. With laser-assist, the experiments showed a 23 and 20 % decrease in cutting force in the feed and machining directions, respectively as well as lower flank wear at similar speeds than traditional machining. It addition, LAML could be used at higher cutting speeds without premature tool chipping that limits traditional machining speed. It was determined that the cutting speed can be increased by 20 % when using LAML compared with traditional milling without reducing the total tool life of the insert.

The study showed that no negatively heat affected zone was created with LAM via optical and SEM microscopy and XRD analysis revealed that there was no detrimental phase change present on the finished workpiece surface. Microhardness analysis showed that hardness did not significantly change through the depth of the workpiece, but only a small decrease on the surface of parts produced by LAML. Residual stress analysis showed approximately 10 % decrease in compressive residual stress for LAML parts compared with traditional machining. The decrease in compressive residual stress measured on the LAML workpiece did not influence workpiece properties of the bulk material and was limited to a shallow layer on the top workpiece surface that was machined by LAML. The differences in surface hardness and residual stress can be directly linked to the heat treatability of the Ti-6Al-4V ELI workpiece.

An economic analysis showed that despite the increased cost of laser equipment and operation, a significant reduction in cost per part and an improvement in material removal rate can be achieved with LAML. Cutting speeds that are limited to 50 m/min

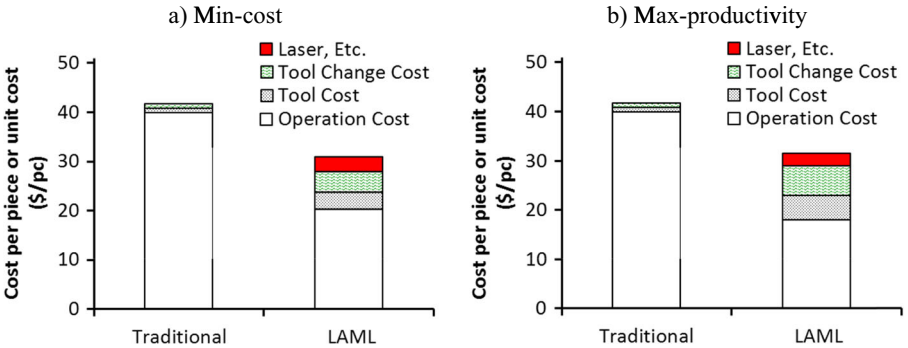

Fig. 16 Economic analysis for optimized cutting conditions—Ti-6Al-4V ELI machining

in traditional milling could be increased to 100 m/min for LAML, and a 33 % reduction in cost can be achieved.

Conflict of Interest The authors hereby confirm that there is no potential conflict of interest, and the research did not involve any Human Participants and/or Animals. The authors also consent to the content and publication of this work.

References

1. Boyer, R., Gerhard, W., Collings, E.W.: Material Properties Handbook Titanium Alloys, ASM International, pp. 483–485 (1994)
2. Donachie, M.J.: Titanium: a Technical Guide, ASM International, Second Ed., pp. 6–11 (1988)
3. Chandler, H.W.: Machining of reactive metals. ASM Handb Mach **10**, 844–857 (1989)
4. Komanduri, R., Reed, Jr., W.R.: Cutting insert with means for simultaneously removing a plurality of chips", US patent US4552492 A (1983)
5. Kuljanic, E., Fioretti, M., Beltrame, L., Miani, F.: Milling titanium compressor blades with PCD Cutter. CIRP Ann Manuf Technol **47**(1), 61–64 (1998)
6. Jawaid, A., Sharif, S., Koksal, S.: Evaluation of wear mechanisms of coated carbide tools when face milling titanium alloy. J Mater Process Technol **99**(1–3), 266–274 (2000)
7. López de Lacalle, L.N., Pérez-Bilbatua, J., Sánchez, J.A., Llorente, J.I., Gutiérrez, A., Albóniga, J.: "Using high pressure coolant in the drilling and turning of low machinability alloys". Int J Adv Manuf Technol **16**(2), 85–91 (2000)
8. Ezugwu, E.O., Da Silva, R.B., Bonney, J., Machado, Á.R.: "Evaluation of the performance of CBN tools when turning Ti–6Al–4 V alloy with high pressure coolant supplies". Int J Mach Tools Manuf **45**(9), 1009–1014 (2005)
9. Rahim, E.A., Sasahara, H.: "High speed MQL drilling of titanium alloy using synthetic ester and palm oil, " Proceedings of the 36th International MATADOR Conference, pp. 193–196 (2010)
10. Sun, J., Wong, Y.S., Rahman, M., Wang, Z.G., Neo, K.S., Tan, C.H., Onozuka, H.: "Effects of coolant supply methods and cutting conditions on tool life in end milling titanium alloy". Mach Sci Technol Int J **10**(3), 355–370 (2006)
11. Bermingham, M.J., Sim, W.M., Kent, D., Gardiner, S., Dargush, M.S.: Tool life and wear mechanisms in laser assisted milling Ti-6Al-4 V". Wear **322–323**, 151–163 (2015)
12. Ding, H., Shin, Y.C.: "Improvement of machinability of Waspaloy via Laser-assisted Machining". Int J Adv Manuf Technol **17**(2), 246–269 (2013)
13. Dandekar, C., Shin, Y.C.: "Laser-assisted machining of a fiber reinforced al-2%cu metal matrix composite". Trans ASME J Manuf Sci Eng **132**(6), 061004 (2010)
14. Dandekar, C.R., Shin, Y.C.: "Experimental evaluation of laser-assisted machining of silicon carbide particle reinforced aluminum matrix composites". Int J Adv Manuf Technol **66**(9), 1603–1610 (2013)
15. Dandekar, C., Shin, Y.C.: "Machinability improvement of Ti6Al4V alloy via LAM and hybrid machining". Int J Mach Tools Manuf **50**(2), 174–182 (2010)
16. Rashid, R.A.R., Sun, S., Wang, G., Dargusch, M.S.: "The effect of laser power on the machinability of the Ti-6Cr-5Mo-5 V-4Al beta titanium alloy during laser assisted machining". Int J Mach Tools Manuf **63**, 41–43 (2012)
17. Rashid, R.A.R., Sun, S., Palanisamy, S., Wang, G., Dargusch, M.S.: "A study on laser assisted machining of Ti10V2Fe3Al alloy with varying laser power". Int J Adv Manuf Technol **74**(1–4), 219–224 (2014)
18. Anderson, M., Patwa, R., Shin, Y.C.: Laser-assisted machining of Inconel 718 with an economic analysis. Int J Mach Tools Manuf **46**, 1879–1891 (2006)
19. Shelton, J.A., Shin, Y.C.: "Laser-assisted micro-milling of difficult-to-machine materials in a side cutting configuration,". J Micromech Microeng **20**(7), 075012 (2010)
20. Shelton, J.A., Shin, Y.C.: "Experimental evaluation of laser-assisted micro-milling in a slotting configuration,". Trans ASME J Manuf Sci Eng **132**(2), 021008 (2010)

21. Ding, H., Shen, N., Shin, Y.C.: Thermal and mechanical modeling analysis of laser-assisted micro milling of difficult-to-machine alloys". J Mater Process Technol **212**(3), 601–613 (2012)
22. Tian, Y., Wu, B.X., Shin, Y.C.: "Laser-assisted milling of silicon nitride and inconel 718". Trans ASME J Manuf Sci Eng **130**, 031013 (2008)
23. Yang, J., Sun, S., Brandt, M., Yan, W.: "Experimental investigation and 3D finite element prediction of the heat affected zone during laser assisted machining of Ti6Al4V alloy". J Mater Process Technol **210**(15), 2215–2222 (2010)
24. Wiedenmann, R., Langhorst, M., Zaeh, M.F.: "Computerized optimization of the process parameters in laser-assisted milling," Lasers in Manufacturing 2011—Proceedings of the Sixth International WLT Conference on Lasers in Manufacturing, Vol. **12**(A), pp. 607–616 (2011)
25. Wiedenmann, R., Liebl, S., Zaeh, M.F.: Influencing factors and workpiece's microstructure in laser-assisted milling of titanium. Laser Assist Net Shape Eng **39**, 265–276 (2012)
26. Brecher, C., Rosen, C., Emonts, M.: "Laser-assisted milling of advanced materials". Physics Procedia **5**(B), 259–272 (2010)
27. Sun, S., Brandt, M., Barnes, J.E., Dargusch, M.S.: "Experimental investigation of cutting forces and tool wear during laser-assisted milling of Ti-6Al-4 V alloy". Proc Inst Mech Eng B J Eng Manuf **225**(9), 1512–1527 (2011)
28. Touloukian, Y.S.: Thermophysical properties research center, purdue university, thermophysical properties of matter; [the TPRC data series; a comprehensive compilation of data]. IFI/Plenum, New York (1970)
29. Hahn, J.D., Shin, Y.C., Krane, M.J.M.: "Laser transformation hardening of Ti-6Al-4 V in solid state with accompanying kinetic model". Surf Eng **23**(2), 78–82 (2007)
30. Vreeling, J.A., Ocelík, V., De Hosson, J.T.M.: "Ti–6Al–4 V strengthened by laser melt injection of WCp particles,". Acta Mater **50**(19), 4913–4924 (2002)
31. Güleryüz, H., Çimenoğlu, H.: "Effect of thermal oxidation on corrosion and corrosion–wear behaviour of a Ti-6Al-4 V alloy,". Biomaterials **25**(16), 3325–3333 (2004)
32. da Silva, S.L.R., Kerber, L.O., Amaral, L., dos Santos, C.A.: "X-ray diffraction measurements of plasma-nitrided Ti–6Al–4 V,". Surf Coat Technol **116–119**, 342–346 (1999)
33. Mantle, A.L., Aspinwall, D.K.: Surface integrity of a high speed milled gamma titanium aluminide. J Mater Process Technol **118**, 143–150 (2001)